[논 문] 한국재료학회지
Korean Journal of Materials Research
Vol. 2, No. 5 (1992)

Ti-24Al-11Nb 합금의 피로균열성장거동에 관한 연구

배 규 식 · 이 문 희
수원대학교 전자재료공학과

A Study on the Fatigue Crack Growth Behavior of A Ti-24Al-11Nb Alloy

Kyoo Sik Bae and Moon Hee Lee
Department of Electronic Materials Department, The University of Suwon, P.O.Box 77, Suwon, Korea

Abstract The mechanisms of fatigue crack growth (FCG) in a Ti_3Al-based (α_2) alloy, Ti-24Al-11Nb (a/o) with acicular microstructure were studied with particular attention focused on the fatigue crack path through the microstructure and on the effects of specimen orientation and crack closure. The results showed that the fatigue cracks of Ti-24Al-11Nb alloy grew much faster than conventional titanium alloys, with little difference in FCG rates for TL and TS orientations. The fatigue crack paths revealed crystallographic transgranular fracture with frequent serrations and branching. This is in agreement with the known effects of slip planarity and microstructure on the FCG behavior. The load-displacement hysteresis loops showed that the crack closure influenced the FCG behavior.

1. Introduction

Considerable effort is being directed toward development of titanium aluminide alloys, based upon the α_2 (Ti_3Al) intermetallic phase, for high-temperature applications in advanced aircraft components. The α_2 intermetallic phase has attractive strength and modulus values, especially when normalized by its low density, but shows limited ductility at ambient temperatures[1-2]. Therefore, alloy development efforts have been focused on improving the balance of strength and room temperature ductility. It has been found that significant additions of Nb to Ti_3Al based alloys, as a β-titanium phase stabilizer, will enhance room temperature ductility. The Ti_3Al-Nb alloy containing about 11 at. % Nb has been shown to have better ductility owing to the increase in non-basal slip activity[3~5].

Number of studies on the mechanical properties of Ti_3Al and Ti_3Al-based alloys have been conducted. But very limited data on the fatigue behavior have been reported in the open literature[3~5], partly due to difficulty in performing fatigue tests on these brittle alloys. More specifically, there is very little information on the microscopic mechanisms of fatigue crack growth (FCG)[4-5], despite that aspects of damage tolerance in titanium aluminides intermetallics have been subjects of considerable interest. The objective of the present investigation was to examine in detail the role of the acicular microstructure on the fatigue crack growth behavior of the Ti_3Al-base alloy, Ti-24Al-11Nb(a/o), at room temperature. Special attention was given to the path of the fatigue crack through the microstructure, fracture mode and the occurrence of crack closure. The FCG behavior of this alloy was compared with those of conventional Ti-6Al-4V and other Ti_3Al-based alloys with similar microstructure. Goals of the work were fundamental understanding of the microscopic fatigue crack growth process in Ti-24Al-11Nb alloy.

2. Experimental

The material used in the study was received

as 33msm thick, extruded bar of an ingot cast alloy. The chemical composition of the alloy was analyzed as Ti/65.3, Al/23.6, Nb/11.0, C/0.17, O_2/0.0042 and H_2/0.21 in atomic percent.

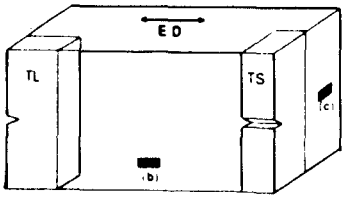

(a)

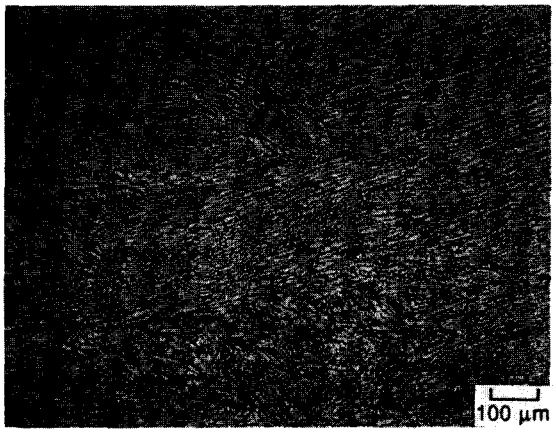

(b)

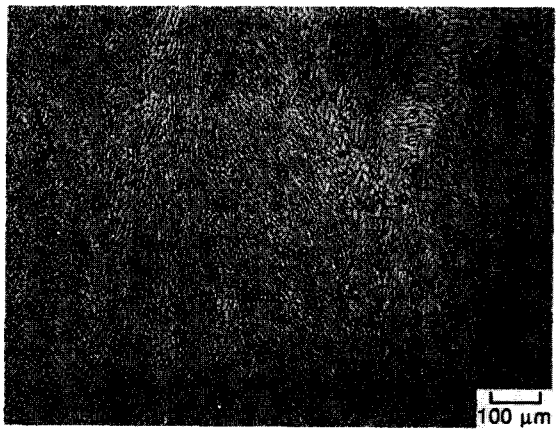

(c)

Fig. 1. Crack path orientation code (a) and microstructures of Ti-24Al-11Nb in (b) longitudinal section and (c) transverse section.

Three-point bend fatigue specimens, 63.5mm ×12.7mm×6.35mm with a 2.5mm deep notch were machinned to give TL or TS orientations, as shown in Fig. 1-a. Notches were made by electro-discharge machining (EDM). One side of each specimen was mechanically polished and etched to observe the crack growth better. Knife edges were glued onto the mouth of each specimen to attach a clip gauge.

Fatigue tests were conducted at room temperature using a computer-controlled, servohydraulic, mechanical test machine at a constant load amplitude at 1 Hz and R=0.1. Data acquisition and reduction were performed automatically by the computer. Crack length was determined from the unloading compliance (50%−90% of the maximum load) and crack growth rate by the secant method at every 0.025mm of crack growth. The equations to compute the crack length and alternating stress intensity were taken from Ref. (6). The effective modulus, 93 GPa (13.5 $\times 10^6$ psi), was calculated from the measured crack lengths and compliances[6]. Crack lengths were also confirmed on the specimen surface by the measurement using a travelling microscope, as a check on the compliance method. Load-displacement hysteresis loops were periodically plotted to measure the amount of fatigue crack closure. The crack paths and fractufe surfaces were examined under optical and scanning electron microscopy.

3. Results and Discussion

The microstructure of the Ti-24Al-11Nb alloy is shown in Fig. 1-b and c. This acicular microstructure is similar to that formed by slow cooling of conventional ($\alpha+\beta$) titanium alloys from the β-phase field[7-8]. As can be seen, long colonies of α_2 (Ti_3Al) are banded in the extrusion direction (ED) (Fig. 1-b). Planes normal to ED exhibit α_2 grains with reduced aspect ratio and somewhat random orientations (Fig 1-c). Similar alignment of elongated α_2 grains in the longitudinal direction of

rolling by hot rolling has been observed for a Ti-25Al-10Nb[9] and γ-TiAl-based alloys[10].

The variation of FCG rate (da/dN) with alternating stress intensity ($\triangle K$) is shown in Fig. 2. For comparison, a FCG curve for the $\alpha+\beta$ Ti-6Al-4V alloy with coarse, lamellar microstructure[7-8] are also included. As can be seen, the fatigue crack growth rate (FCGR), da/dN is higher than that of conventional Ti-6Al-4V by an order of magnitude at imposed $\triangle K$, showing brittle nature of the Ti-24Al-11Nb alloy. This FCGR is, however, comparable to those of forged Ti_3Al-based alloys[4-5] with similar microstructure. It is also noted from Fig. 2 that the fatigue regime from $\triangle K_{th}$ to the final fracture spans less than 10MPa $m^{1/2}$. The maximum K value sustained by the present materials was about 15, compared to 17-21 MPa $m^{1/2}$ for the other Ti_3Al-based alloys[4-5]. A fracture toughness test on the present TS specimen showed the K_{Ic} to be 17MPa $m^{1/2}$, showing that the maximum K value approximated the K_{Ic}. Shorter fatigue regime for the present test is seen associated with the low test frequency (1 Hz) compared to 20 Hz for other studies[4-5], because the moist air can embrittle a variety of Ti alloys and Ti_3Al intermetallics, especially with acicular microstructure[5,11]. It has been indeed shown that lowering the frequency from 20 to 1 Hz for the Ti-25Al-10Nb alloy[5] in the room temperature moist air environment caused the FCGR to increase by an order of magnitude in the Paris regime.

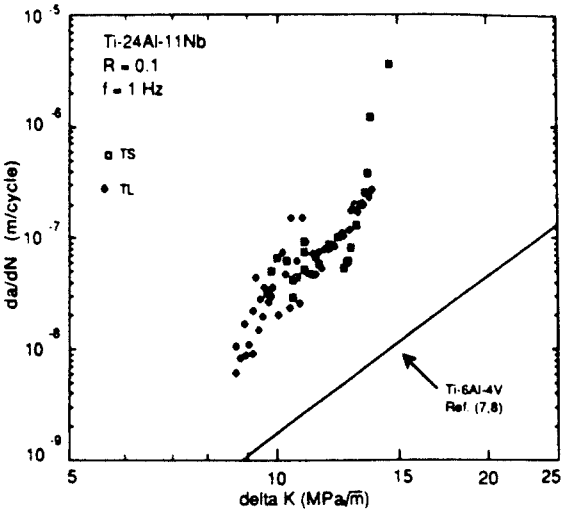

Fig. 2. Log da/dN vs. log $\triangle K$ plots of Ti-24Al-11Nb tested in TL and TS orientations.

Fig. 2. also shows that there is little difference in the FCGR between TL and TS orientations. It is well known that the yield strength, work hardening behavior and the slip characteristics of Ti alloys are related to several microstructural parameters such as colony size, the orientation of the colony to the stress axis and the crystallography of slip[12~15]. In a study of the deformation behavior of a Ti-8Al-1Mo-1V alloy, Chan et al.[12] observed that the predominant slip system was dependant on the colony orientation with respect to the stress axis. The colony boundaries in the Ti-6Al-4V alloys were observed to act as a major barrier to slip[13]. These deformation characteristics are also evident for the present Ti-24Al-11Nb alloy, as can be seen from the micrograph of the crack path shown in Fig. 3. The FCG occurred mostly in α_2 grains, contray to the observation in Ref. (5). Cracking is generally transgranular and show tortuous crack paths with frequent branching and serrations (Fig. 3-a and b). Serrations occur more frequently in the regions where the long axis of acicular grains aligns roughly perpendicular to the crack growth direction. At higher magnification (Fig. 3-c), even relatively straight crack segments in Fig. 3-b can be seen to contain small scale "zigzags". It is known that the principal mode of deformation within the α_2 phase is planar slip[4,5,16]. Hence, fatigue crack in the present Ti-24Al-11Nb alloy grows straight along specific crystallographic direction on the slip plane in a α_2 colony[5] and changes its direction when traversing colony boundary, creating zig-zag profiles. Hence, the

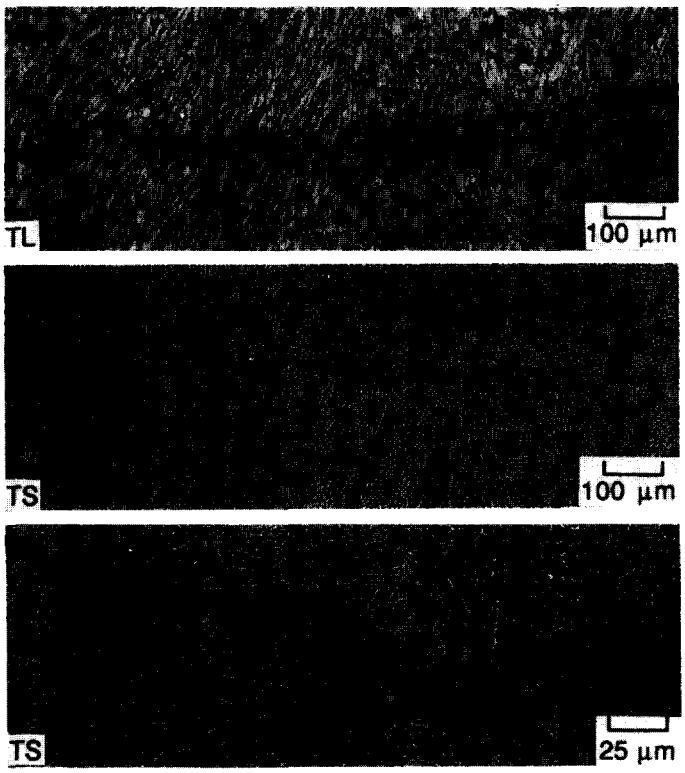

Fig. 3. Optical micrographs, showing fatigue crack paths at $\triangle K$ (MPa $m^{1/2}$) of (a) 8.2 to 10.3 (TL), (b) 8 2 to 10.3 (TS) and (c) 11.0 to 11.7 (TS). Crack growth direction is from left to right.

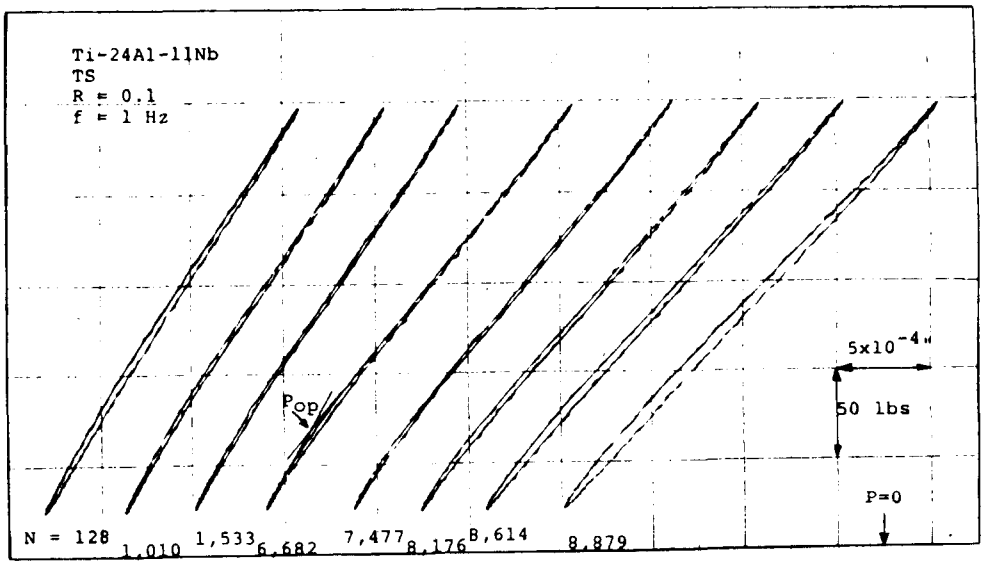

Fig. 4. Hysteresis loops as a function of number of cycles, showing the occurrence of fatigue crack closure.

FCGR is expected to be lower in TS than in TL orientation as have been observed for a Ti-6Al-4V alloy[14,15], since fatigue crack on TS-oriented specimens has to pass more colony boundaries and change its direction more frequently. But the FCGR was the same for both orientations as shown in Fig. 2. It appears that the favorable effects of periodic deflections at the colony boundaries are negated by the weak resistance of the very brittle α_2 colony to crack growth.

Large-scale crack branchings such as in Fig. 3-b were occasionally observed through the travelling microscope. The branching indeed decreased the FCG rates momentarily owing to reduced effective $\triangle K$. In addition, metal fragments were observed to form between the main and branched cracks, which were believed to have acted as wedges, creating irregular load-displacement hysteresis loops on a X-Y recorder. It is thus viewed that local crack branching retards the FCG in the α_2 alloy, although its effects are again negated by fast brittle fracture.

Crack branching and serrations produce a rough fracture topography and in turn cause a roughness-induced closure[7,8,16,17]. In other word, opposing crack face load bearing contact can exist with a tortuous fatigue crack path which will reduce the $\triangle K$ experienced at the crack tip, and thus increase the necessary applied $\triangle K$ to achieve crack extension. Fig. 4 shows a typical example of load-displacement hysteresis loops for a TS specimen. The crack opening load P_{op} was taken from hysteresis loops, when a change in compliance occurred[6]. The ratio P_{op}/P_{max}, where P_{max} is the maximum load, was as high as 0.3. This demonstrates that crack closure plays an important role for the FCG in α_2 alloy as in other planar slip materials, especially at the fatigue threshold region as have been observed for a Super Alpha 2 (Ti-Al-Nb-V) alloy[4]. In this connection, oxide-induced closure in relation with the moist air embrittlement previously discussed can not be ruled out to operate in the present α_2 alloy.

Fractography supports above observations of the effect of colony orientation, crystallographic crack growth in α_2 colony, deflection at colony boundaries and branching on the FCG processes in Ti-24Al-11Nb alloy. A low magnification fracture surface is shown in Fig. 5. The fatigued area is somewhat smooth, yet with locally rough regions, as compared to the

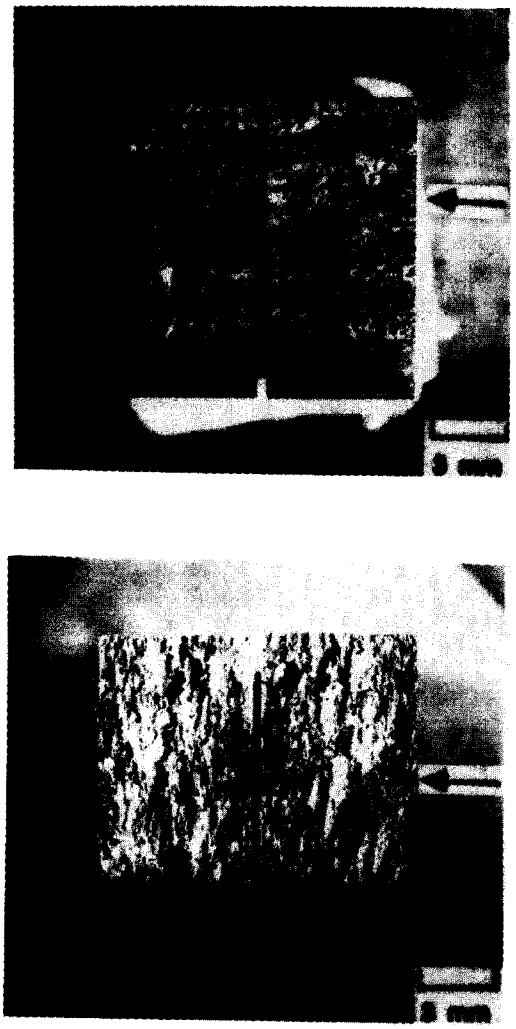

Fig. 5. Low magnification optical micrographs of fracture surfaces in (a) TL and (b) TS orientations. Arrows indicate boundaries between fatigue and final fracture regions.

final rupture surface. But the boundary between two regions is still unclear. The TL specimen reveals slightly rougher region of FCG than the TS specimen. The fatigue crack fronts appear highly irregular. To be noted is that fibrous fracture patterns run parallel and perpendicular to the crack growth direction of TL and TS orientations, respectively. This difference is related to the different orientation of elongated colony structure with respect to crack growth direction. Typical SEM micrographs of fracture surfaces shown in Fig. 6-a reveals transgranular cleavage fracture probably on crystallographic planes, consisting of river patterns and secondary cracks (branching). Regions having a more rounded appearance, indicative of limited plasticity[4] were also observed, as shown in Fig. 6-b. The crack front changes its propagation directions across colony boundaries creating zig-zag profiles (Fig. 6-b).

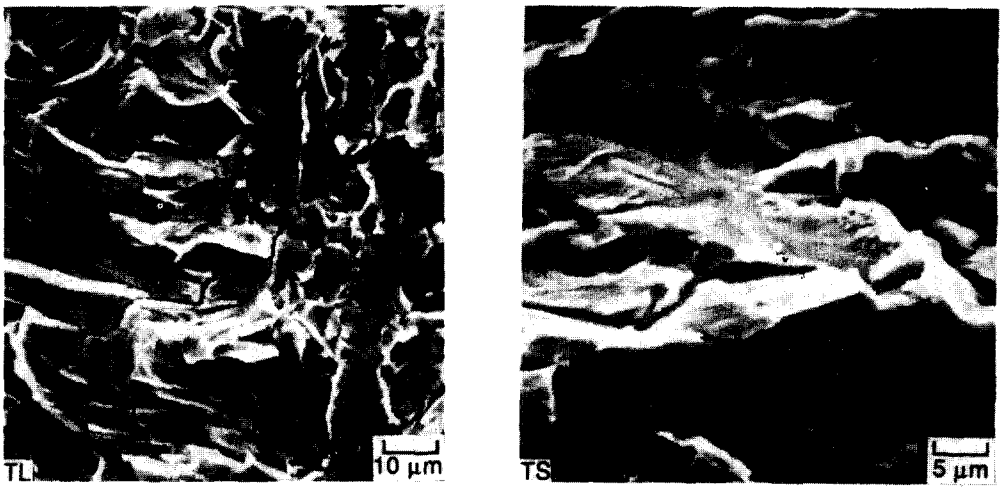

Fig. 6. SEM micrographs of fracture surfaces at $\triangle K$ (MPa $m^{1/2}$) of (a) 9.9 (TL) and (b) 9.7 (TS). Crack growth direction is from bottom to top.

4. Conclusions

1) Compared to the FCGR of the conventional Ti-6Al-4V, that for Ti-24Al-11Nb alloy was much higher for a given $\triangle K$. Despite the addition of Nb, the present Ti_3Al-based alloy exhibited limited ductility. Shorter fatigue regime from threshold to the final fracture for the present test compared to others with Ti_3Al -based alloys were attributed to the embrittlement induced by the moist air in association with low test frequency.

2) The fatigue crack paths showed crystallographic transgranular fracture in α_2 colonies with frequent serrations and branching. Effects of crack impediment and crack deflection at colony boundaries appear to be negated by the weak resistance of the very brittle α_2 colony structure to crack growth, resulting in little difference in FCGR for TL and TS orientations.

3) The crack closure occurred as a result of rough fracture surfaces induced by serrations and branching. Oxide-induced closure may also operate.

4) In support of above observations, fracture surfaces revealed fibrous pattern parallel and perpendicular to the crack growth direction in TL and TS orientation respectively as a result of banded colonies along ED, and

transgranular cleavage fracture consisting of river-like patterns, secondary cracks and zig-zag profiles.

References

1. H. A. Lipsitt, D. Shechtman and R. E. Schafrik, Met. Trans. **11A**, 369 (1980)
2. H. A. Lipsitt, Proc. of MRS, *High-Temp. Ordered Intermetallic Alloys*, ed., by C. C. Koch, C. T. Lin and N. S. Stoloff, 351 (1985).
3. M. Yamaguchi and Y. Umakoshi, Prog. in Mat. Sci. **33**, 1 (1989)
4. D. L. Davidson, J. B. Campbell and R. A. Page, Met. Trans., **22A**, 377 (1991)
5. P. B. Aswath and S. Suresh, Met, Trans. **22A**, 817 (1991)
6. ASTM E813, "J_{Ic}, A Measure of Fracture Toughness".
7. G. T. Gray 111 and G. Luetjering, *Titanium Science and Technology*, Vol. 4, ed., by G. Luetjering, U. Zwicker and W. Bunk, 2251 (1984).
8. M. Peters, K. Welpmann and H. Doker, ibid., 2267 (1984).
9. W. P. Hon, S. K. Wu and C. H. Koo, Mat. Sci. & Eng., **A131**, 85 (1991)
10. J. Seeger, A. Bartels and H. Mecking, Scripta Met., **25**, 2523 (1991)
11. G. Luetjering and A. Gysler, *Titanium Science and Technology*, Vol. 4, ed. by G. Luetjering, U. Zwicker and W. Bunk, 2065 (1984).
12. K. S. Chan, C. C. Wojcik and D. A. Koss, Met. Trans., **12A**, 1899 (1981)
13. F. S. Lin, E. A. Starke, Jr., S. B. Chakrabortty and A. Gysler, Met. Trans., **15A**, 1229 (1984)
14. A. W. Bowen, Proc. of 3rd Int'l Conf. on the Strength of Metals and Alloy, Cambridge, U. K., Vol. 1, 446 (1973)
15. C. A. Stubbington, AGARD Conf. Proc., No 185, 3-1
16. R. D. Carter, E. W. Lee, E. A. Starke, Jr and C. J. Beevers, Met. Trans. **15A**, 555 (1984)
17. M. D. Holliday and C. J. Beevers, Int'l J. of Fract., **15**, R27 (1979)